fluids

MDPI

Article

Injectable Composite Systems of Gellan Gum:Alginate Microparticles in Pluronic Hydrogels for Bioactive Cargo Controlled Delivery: Optimization of Hydrogel Composition based on Rheological Behavior

Henrique Carrêlo, André R. Escoval, Paula I. P. Soares *, João P. Borges * and Maria Teresa Cidade *

CENIMAT/i3N, Department of Materials Science, NOVA School of Science and Technology (FCT NOVA), Campus de Caparica, 2829-516 Caparica, Portugal

* Correspondence: pi.soares@fct.unl.pt (P.I.P.S.); jpb@fct.unl.pt (J.P.B.); mtc@fct.unl.pt (M.T.C.)

Abstract: Due to the high complexity of some treatments, there is a need to develop drug-delivery systems that can release multiple drugs/bioactive agents at different stages of treatment. In this study, a thermoresponsive injectable dual-release system was developed with gellan gum/alginate microparticles (GG:Alg) within a thermoresponsive Pluronic hydrogel composed of a mixture of Pluronic F127 and F68. The increase in F68 ratio and decrease in F127 lead to higher transition temperatures. The addition of the GG:Alg microparticles decreased the transition temperatures with a linear tendency. In Pluronic aqueous solutions (20 wt.%), the F127:F68 ratios of 16:4 and 17:3 (wt.%:wt.%) and the addition of microparticles (up to 15 wt.%) maintained the sol–gel transition temperatures within a suitable range (between 25 °C and 37 °C). Microparticles did not hinder the injectability of the system in the sol phase. Methylene blue was used as a model drug to evaluate the release mechanisms from microparticles, hydrogel, and composite system. The hydrogel delayed the release of methylene blue from the microparticles. The hydrogel loaded with methylene blue released at a faster rate than the microparticles within the hydrogel, thus demonstrating a dual-release profile.

Keywords: hydrogels; thermoresponsive; Pluronic; alginate; gellan gum; rheology

Citation: Carrêlo, H.; Escoval, A.R.; Soares, P.I.P.; Borges, J.P.; Cidade, M.T. Injectable Composite Systems of Gellan Gum:Alginate Microparticles in Pluronic Hydrogels for Bioactive Cargo Controlled Delivery: Optimization of Hydrogel Composition based on Rheological Behavior. *Fluids* **2022**, *7*, 375. https://doi.org/10.3390/fluids7120375

Academic Editor: Mehrdad Massoudi

Received: 31 October 2022
Accepted: 2 December 2022
Published: 6 December 2022

1. Introduction

With the significant developments of the last few decades in biomedicine, a great focus has been on the design and development of drug-delivery systems (DDSs). These systems are used to deliver drugs/bioactive agents to the human body in a controllable and sustainable way that is adequate for the desired treatment. These can be designed using multiple forms, such as nanoparticles, microparticles, hydrogels, liposomes, and others [1–3]. These systems can be designed to deliver different types of drugs and can also be designed for in situ delivery. Introducing a DDS that can deliver more than one bioactive agent in loco is of great interest for many applications. Due to the high complexity of different types of treatments, a DDS that can adapt its release to the needs of the particular case can present better results than a simple direct administration of pharmaceutical agents. The release of more than one drug at different stages of the treatment will allow synergistic treatment. Ma et al. [4] developed a sequential delivery system that can deliver different types of drugs at different stages of the wound-healing process. The system was composed of a sodium alginate/bioactive glass (45S glass) injectable hydrogel [5] with sodium alginate microparticles with a conditioned medium of cells. In addition, polylactic-co-glycol acid (PLGA) microparticles loaded with pirfenidone were loaded into the system. The hydrogel would rapidly release bioglass ionic products to regulate the inflammatory response. Then, the microparticles would release the conditioned medium to facilitate the formation of vascularized granulation tissue. Lastly, the PLGA microparticles

would release pirfenidone to prevent scar formation and enhance skin regeneration. In another study, Li et al. [6] developed an implantable fiber structure device that offered a dual release of doxorubicin (Dox) and angiogenesis inhibitor apatinib (Apa) for breast cancer treatments. This device had the objective of rapidly releasing Dox, followed by a more sustained release of Apa to prevent tumor recurrence. Thus, this system could treat and prevent tumor recurrence. In cancer treatments, sequential and dual-delivery systems can have great benefits [7].

The development of microparticles that can be used as DDSs has been the topic of many studies. Microparticles made with natural polysaccharides such as alginate and gellan gum are an attractive topic since these materials are biocompatible and biodegradable. Alginate is a known anionic polysaccharide commonly used in biomedicine [8]. Gellan gum is also an anionic polysaccharide that has good mucoadhesive properties [9]. Gellan gum has higher tensile stress than alginate, although it is not as ductile [10]. The mixture of these two materials allows for the production of different DDS with adjustable properties. Since they are both sensitive to ionotropic gelation, especially to the presence of divalent cations, such as Ca^{2+}, it is possible to produce different hydrogel DDS from their blend. This mixture has been previously used to produce microparticles that could be used in different biomedical applications [9,11,12], including drug delivery [13].

Hydrogels are three-dimensional (3D) structures that can accumulate great quantities of water within their structure [14,15]. Consequently, hydrogels can store large amounts of drugs/bioactive agents to be released within the human body. Hydrogels can be sensitive to different stimuli. Thermoresponsive hydrogels are hydrogels that undergo a physico-chemical change triggered by temperature differences [16–19]. Pluronic (or poloxamer) is one example of a thermoresponsive hydrogel. It is composed of poly(ethylene oxide) (PEO) and poly(propylene oxide) (PPO) in a triblock structure (PEO-PPO-PEO). In an aqueous solution at low temperatures, it is within its sol state. Then, with increasing temperature, a micellar structure starts to form, due to an increase in the hydrophobicity of PPO, leading to the formation of a micellar gel [20]. Due to this capability, Pluronic hydrogels can be used as injectable DDSs. The hydrogel at operating room temperature (21 °C) can be in the sol state, thus facilitating its injectability, and with injection to the human body, gelation occurs in situ due to the physiological 37 °C. Within the human body, the hydrogel releases its components at a rate dependent on the hydrogel structure and drug affinity. To inject it into the human body, a rheological characterization should be performed to understand the transition temperature of the hydrogel. This transition temperature should be above 25 °C and less than 37 °C [16,21]. In the market, there are different types of Pluronic, such as F127 ($PEO_{99}PPO_{69}PEO_{99}$) and F68 ($PEO_{80}PPO_{27}PEO_{80}$). These two differ in the ratio of PEO and PPO [22]. Their mixture has been previously studied and it was found that their combination can regulate the transition temperature [22,23].

To have a dual-release pattern, it is possible to introduce microparticles with different release patterns within the hydrogel. These microparticles can be developed to deliver drugs in a more prolonged way. Thus, a microparticle–hydrogel injectable DDS can be produced [24]. With this DDS, it is possible to load drugs/bioactive agents within the hydrogel and within the microparticles. The drugs loaded within the hydrogel will be released in an earlier stage. Afterwards, the microparticles would release the drugs in a more prolonged release. These dual-release platforms can serve as a DDS that can be used in more complex treatments that require more than one drug. In addition, it is possible that the hydrogel delays the release profile of the microparticles [24].

However, introducing microparticles within the hydrogel can alter the rheological properties of the hydrogel. Previous studies have found that the presence of microparticles changes the transition temperature of hydrogels [16], so it is important to define and adjust the transition temperature of the microparticle–hydrogel composite system. To this end, in this article gellan gum/alginate microparticles, which had been previously optimized [25], were introduced within a Pluronic hydrogel to develop an injectable DDS. In a previous study, the microparticles were revealed to have adequate drug-delivery capabilities using

methylene blue as a model drug [25]. Two types of Pluronic (F127 and F68) were used to control the transition temperature of the hydrogel. Then, different concentrations of microparticles were used to study their impact on the hydrogel's rheological characteristics. With this, it was possible to study the effect of the ratio of Pluronic F127:F68 and the effect of microparticle concentration in the DDS. In vitro drug-delivery tests were performed to understand how the hydrogel affects the release profile from microparticles and how the microparticles affect the release profile from hydrogel.

2. Materials and Methods

2.1. Materials

Pluronic F-127 and Pluronic F68 were purchased from Sigma Aldrich (St. Louis, MO, USA). High-acyl gellan gum was purchased from Sigma-Aldrich (USA) as Phytagel. Alginic acid sodium salt was purchased from BioChemica (Panreac Química SLU, Castellar del Vallès, Spain). Methylene blue (MB), in powder form, was purchased from Alfa Aesar (Haverhill, MA, USA), and calcium chloride from Carl Roth (Karlsruhe, Germany). The phosphate buffer solution (PBS) was prepared with two different pH: 7.4 and 6.5. For pH 7.4, the following reagents were added to 800 mL of Millipore water: 4 g of sodium chloride (NaCl 100%) (J. T. Baker, Avantor, USA), 0.1 g of potassium chloride (KCl $\geq$ 99%) (Sigma-Aldrich, USA), 0.72 g of disodium hydrogen phosphate (Na_2HPO_4) (Panreac Química SLU, Spain) and 0.12 g of potassium dihydrogen phosphate (KH_2PO_4) (Panreac Química SLU, Spain). Then, more Millipore water was added to make 1 L of solution. For PBS with pH 6.5, the quantities of each reagent were as follows: 8 g of NaCl, 0.2 g of KCl, 0.61 g of Na_2HPO_4 and 0.19 g of KH_2PO_4.

2.2. Microparticle Production

Gellan gum/alginate microparticles were produced via a coaxial air flow method. This method used optimized production parameters that were obtained in a previous study [25]. A solution made with 2 wt.% of a mixture of alginate and gellan gum (ratio of 50:50) was prepared. Then, using the coaxial air flow method, microparticles were ionically cross-linked in a gelation bath of calcium chloride solution (3.5 w/v%). Dried microparticles had a size between 150 and 220 µm, and in their swollen state they reached diameters of around 400 µm.

2.3. Hydrogel and Microparticle–Hydrogel Composite System

Pluronic F127 and F68 were mixed into an aqueous solution (20 wt.%) with different ratios of F127 and F68 (F127:F68 14:6, 15:5, 16:4, 17:3, 18:2, and 20:0). After mixing, the solutions were stored at 4 °C to let the Pluronic dissolve and to maintain the hydrogel in the sol state. The microparticle–hydrogel solutions were prepared by mixing different concentrations of dried microparticles within the hydrogel in the sol state. Microparticles were mixed with concentrations of 2%, 5%, 10% and 15% (wt.%).

2.4. Rheological Characterization

The rheological characterization was performed with an Anton Paar MCR 501 rheometer, with a plate/plate geometry of 50 mm of diameter (PP50) and a gap of 3 mm. This gap size was chosen due to the size of the microparticles and to avoid confinement issues. The high gap, however, did not give rise to any measurement problems indicated by the software. All oscillatory regime tests were carried out within the linear viscoelastic region of the hydrogel. The sol–gel transition was determined with temperature sweeps at a single angular frequency (1 rad/s). The temperature sweeps were performed from 15 to 50 °C, with 1 °C/min. Frequency sweeps were carried out within a range of 1 to 100 rad/s at 37 °C. To understand the possibility of injectability, flow curves were carried out between 1 to 1000 s^{-1} at 21 °C (surgery room temperature [26]) following Cezar et al. [21]. Three replicas were used for each measurement.

2.5. In Vitro Degradation of Pluronic

To understand how the Pluronic hydrogel degrades within a PBS solution, Pluronic solutions with an F127:F68 ratio of 17:3 were introduced in a recipient made from a dialysis membrane. Then, the recipients were kept at 37 °C in the gel state. Finally, these recipients were added to 50 mL PBS solutions with pH of 6.5 and pH 7.4 at 37 °C. At different times—1 h, 3 h, 6 h, and 24 h—the recipients were taken out of the PBS and its content was analyzed in the rheometer, with frequency sweeps. Four replicas were used for each measurement.

2.6. In Vitro Drug Release

To characterize the release profiles of the microparticle–hydrogel composite system and the hydrogel alone, MB was encapsulated in microparticles according to our previous work [25]. Microparticles were left for 4 days in a PBS (pH 7.4) solution with 290 µg/mL of MB. After this, they were removed from the solution, washed, and dried.

The hydrogel with MB was prepared by mixing MB in the Pluronic solution in the sol state. The used hydrogels had F127:F68 ratios of 17:3 and 16:4. Within a recipient made from a permeable membrane, batches of microparticle–hydrogel composite systems were introduced with 2 wt.% and 5 wt.% of microparticles. The amount of microparticles did not change, being always 0.02 g of MB-loaded microparticles. To make the 2 wt.% and 5 wt.% systems, the volume of the hydrogel was adapted.

The MB release from plain hydrogel was conducted by filling the recipient with 2 mL of MB-loaded Pluronic (17:3) in the sol state. Then, the recipients with the membranes were submerged in 10 mL of PBS solutions with pH 6.5 and pH 7.4. PBS solutions were kept at 37 °C with orbital agitation. At regular periods (0, 0.25, 1, 3, 6, 24, 48, 72, 144, 192, 240 and 312 h), 2 mL of the PBS was retrieved and replaced with fresh PBS. The 2 mL was then analyzed by UV-vis spectroscopy (PG Instruments Ltd., Lutterworth, UK) using a calibration curve to determine the MB concentration at each time. Five replicas were used for each measurement. With these results, different mathematical models were used to fit the experimental data of the release profiles.

3. Results and Discussion

3.1. Sol–Gel Transition Temperature

Figure 1 depicts temperature sweeps in oscillation that give the transition temperatures of different ratios of Pluronic F127:F68 in an aqueous solution (20 wt.%). Three regions can be identified. The first region is the sol region, where the hydrogel is in the sol state, where $G'' >> G'$ with very low values of G'. This indicates that the system is in the sol state with viscous behavior. This region stops with the sharp increase of G' and G'' at a specific temperature, that hereby we will designate Ti (initial temperature). In this second region, micellization starts to occur, and a structure made from the interaction of the micelles starts to appear. A structured form of the hydrogel is fully reached at a temperature where both moduli reach a plateau, which we will designate Tp (temperature plateau) [22,27], leading to the third region. This plateau indicated the formation of a stable micellar structure independent of temperature within the studied ranges, where $G' > G''$ had values significantly higher than the moduli below Ti. These two temperatures sol–gel indicate the sol–gel transition temperatures, where the Tp is the temperature at which the transition fully occurs. Suman et al. [28] studied Pluronic F127 transition from the sol to the gel and to an attractive glass state. Above the micellization temperature, the loose chains of PEO-PPO-PEO start to join and form micelles, resulting in a phase where micelles and loose chains coexist. With increasing temperature, the loose chains start to form micelles until a point that there are almost no loose chains in the system. After the saturation of micelles, they start to aggregate more, and a more favorable interaction between micelles begins, leading to a structure formation. Depending on the concentration, the size of micelles might increase; however, with more concentrated solutions, the loose chains form more micelles, leading to faster structural formation. This structure leads to the formation of an

attractive (due to the interactions between micelles) glass state. With higher temperatures, the structure of the hydrogel collapses.

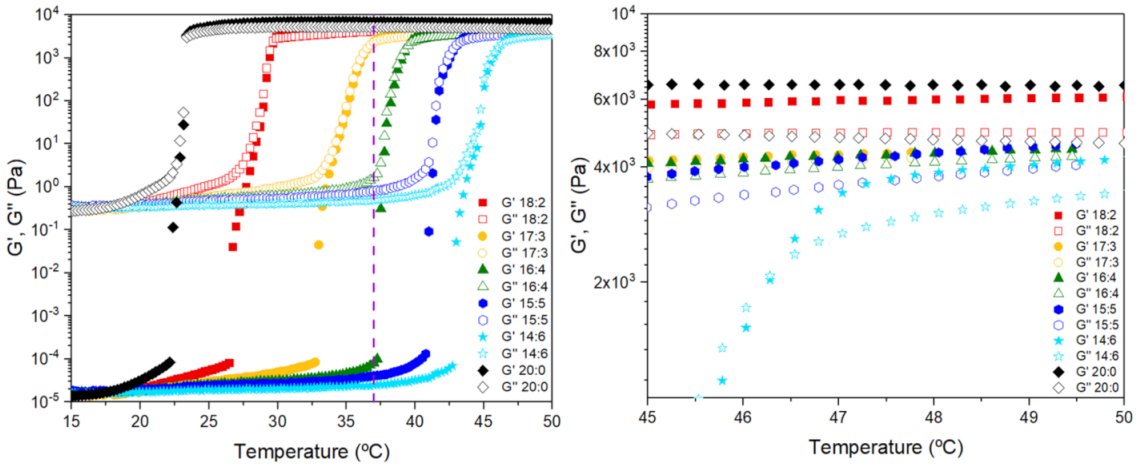

Figure 1. Elastic (G′) and viscous (G″) moduli of different ratios of Pluronic F127 and F68, of a Pluronic aqueous solution of 20% (wt.%) (**left**). The violet line represents 37 °C. On the (**right**), there is an approximation of the region between 45 and 50 °C of the image on the left.

For this work, the ideal injectable system has the sol–gel transition temperature between 25 °C and 37 °C. This allows the system to be in the sol phase at operating room temperature [26] (around 21 °C) and the gel phase at body temperature (37 °C). The transition temperatures increased with a decrease of F127 and with an increase of F68. For example, with a Pluronic ratio of 20:0, the Tp was 23.62 ± 0.11 °C, while with a ratio of 14:6, the Tp increased more than 20 °C, to a Tp of 45.81 ± 0.11 °C. This is due to the decrease in F127 percentage and increase in F68 presence within the hydrogel. In this hydrogel, F127 is the phase that has the highest concentration and is the one that micellizes. Pluronic F68 does not form a micellized phase at these concentrations. In addition, Pluronic F68 has a much higher gelation temperature than Pluronic F127 [22,29]. This is because Pluronic F127 ($PEO_{99}PPO_{69}PEO_{99}$) has more PPO content than F68 ($PEO_{80}PPO_{27}PEO_{80}$). The thermoresponsivity of Pluronic hydrogels is controlled by the PPO content [30]. With increasing temperature PPO becomes hydrophobic. Thus, with more PPO moieties, the transition temperature decreases. Decreasing the F127 concentration, there will be fewer chains of the phase that can form the micellized structure. In addition, since F68 is a phase that does not form micelles in these concentrations [31] and its chains will be between the micelles of the F127, this can also delay the interactions between F127 micelles. Thus, with the change in the ratio of these two Pluronic types, it is then possible to change the transition temperatures to ranges that are suited for injectable systems. In this study, ratios of 17:3 and 16:4 had their sol–gel transition temperatures within a range close to 37 °C.

3.2. Sol–Gel Transition of the Microparticle–Hydrogel Composite System

Figure 2 shows the effect of microparticles on the different Pluronic F127:F68 ratios. In all Pluronic F127:F68 ratios, microparticle presence decreased the transition temperatures. Increasing the microparticle concentration further decreased the transition temperature. With 2% of microparticles, the hydrogel decreased the Tp between 0 and 1.81 °C, whilst with 15% the Tp decreased between 6.7 (for a ratio 18:2) and 7.25 °C (for a ratio of 14:6). This decrease might be explained by the swelling of the microparticles within the Pluronic solution leading to Pluronic concentration increase [16,32]. In addition, changes in Ti may have been due to the interaction of the carboxylic groups of alginate and gellan gum with the ether groups of Pluronic. These interactions might prompt the formation of a gel structure [16,33].

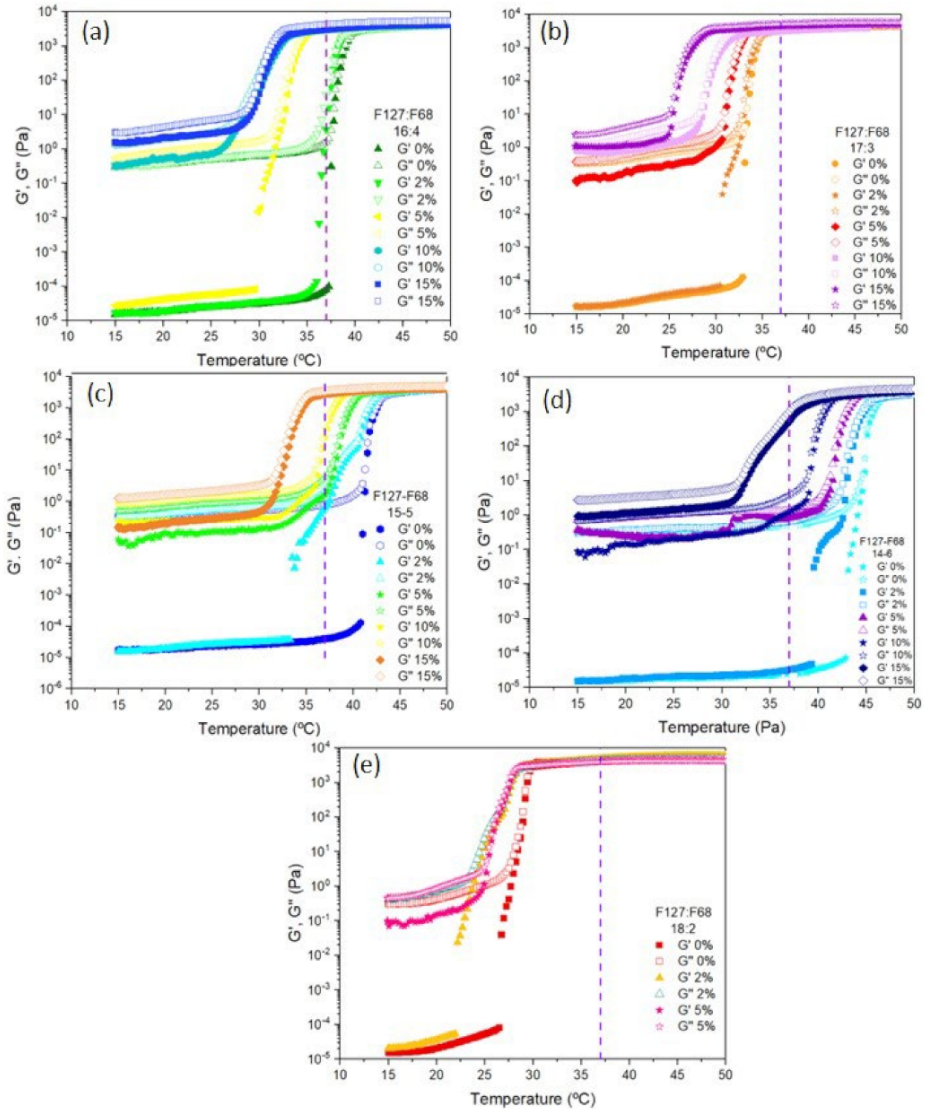

Figure 2. Elastic (G′) and viscous (G″) moduli of different microparticle concentrations (in w/w%) within Pluronic F127:F68 ratios of (**a**) 16:4; (**b**) 17:3; (**c**) 15:5; (**d**) 14:6; (**e**) 18:2. The violet dotted line represents 37 °C.

In the sol state, the microparticles increased in both moduli. In all microparticle concentrations, G″ was significantly above G′, indicating viscous behavior of the sample. From 5% to 15% of microparticles, G′ increased significantly, but remained below G″, and thus the introduction of microparticles gave a more elasticity to the sol state. The moduli had a small slope with the temperature at their sol state, with the moduli increasing with temperature. This might be due to the formation of some micelles within the solution. When the hydrogel reached Ti, the moduli suddenly increased several orders of magnitude until they reached Tp. Above Tp, the moduli stabilized in a plateau with the fully micellized and ordered structure of the Pluronic. With the introduction of microparticles, the moduli increased but G″ remained over G′. Although G″ > G′, the system maintained the gel structure. Within the studied range of frequencies, the same phenomenon was observed. This unexpected phenomenon might be attributed to the interaction between the microparticles. The introduction of the microparticles leads to a more structured system, hence the moduli increase. G″ increase to G″ > G′ might be attributed to the increase in friction between the particles. This friction leads to energy dissipation that contributes to G″ [34,35]. This is corroborated by the fact that with an increase in microparticles, there is an increase in the distance between G″ and G′, due to higher interaction between microparticles. This

effect has been reported in previous studies that used similar rheological tests [35]. Figure 3 shows the Pluronic with a 17:3 ratio in the sol state at 21 °C (Figure 3a), in the gel state at 37 °C (Figure 3b) and in the gel state with the microparticles loaded (Figure 3c).

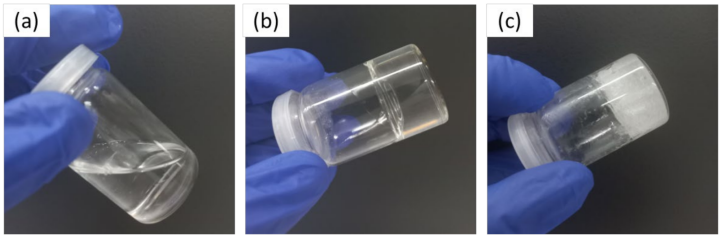

Figure 3. Images of Pluronic F127:F68 at 17:3 ratio: (**a**) 0 wt.% of microparticles at 21 °C, (**b**) 0 wt.% microparticles at 37 °C and (**c**) 15 wt.% microparticles at 37 °C.

Figure 4 presents the variation of the transition temperatures with microparticle concentration and Pluronic F127:F68 ratio. As was previously observed, the decrease in F127 and increase in F68 led to higher transition temperatures. As is observed in Figure 3a, the variation of the studied Pluronic F127:F68 ratios altered the transition temperature more significantly than with the studied microparticle concentrations. Increasing the microparticle concentration led to Tp and Ti decrease (Figure 3b,c, respectively). The microparticles' effect and the Pluronic ratio's effect had no interaction. Regardless of the Pluronic ratio, microparticles led to a constant decrease in Tp at a constant rate. Ti also decreased almost linearly with microparticle presence.

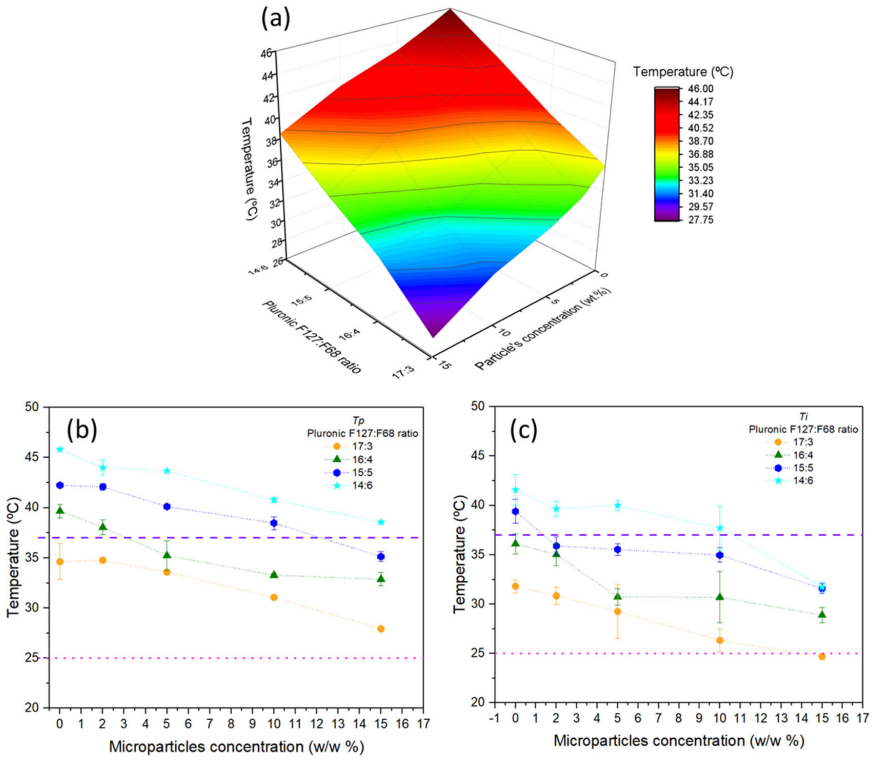

Figure 4. (**a**) 3D representation of the sol–gel transition temperatures (Tp) of the microparticle–hydrogel composite system with variation of Pluronic F127:F68 ratio and microparticle concentration; (**b**) variation in the Tp of the microparticle–Pluronic hydrogel composite system with microparticle concentration at different ratios of F127:F68; (**c**) similar graphic depiction for Ti. In (**b**) and (**c**), the dashed line in purple represents the 37 °C limit, and the dotted line in pink represents the ambient temperature of 25 °C.

Mathematical Fittings of the Transition Temperatures

Mathematical fittings from the obtained transition temperatures (Figure 4b,c) were done to understand the correlation between the concentration of the microparticles and the sol–gel transition temperatures. A linear regression was performed on the obtained Tp and Ti following Equation (1):

$$T = m \cdot c + T_0 \quad (1)$$

T is the transition temperature, which is represented by Tp and Ti (°C), m is the slope of the linear regression, c is the microparticle concentration and T_0 is the intercept, i.e., the transition temperature of the Pluronic solution without microparticles. R^2 is the adjusted error. Linear regression was calculated for each ratio.

Table 1 displays the obtained parameters of the linear fits applied to the experimental data. Regarding Tp, the Pluronic ratios did not influence the effect of the microparticle concentration, since all slopes were similar. Regarding the fittings, all ratios had good R^2 except the ratio of 16:4, but still with a high value. For Ti, the obtained slopes were not as similar between the Pluronic ratios as the slopes of Tp. The obtained R^2 revealed that the linear relationships are not as strong as in Tp. This might be associated with the higher dispersibility attributed to the start of the micellization that was registered during the rheological studies of Ti, as may be observed in Figure 3 (right). The obtained T_0 were similar to the obtained transition temperatures of the ratios without microparticles (0 w/w%), indicating a good model that describes the effect of microparticle concentration on the transition temperatures.

Table 1. Linear regression of the obtained transition temperatures according to microparticle concentration (wt.%). Left table for Tp and right table for Ti. m is the slope of the regression and T_0 is the intercept, i.e., the modeled temperature with 0 wt.%.

Tp			
F127:F68 Ratio	***m* (°C/(wt.%))**	***T*$_0$ (°C)**	***R*^{2}**
14:6	–0.4658	45.55	0.9799
15:5	–0.4762	42.66	0.9764
16:4	–0.4564	38.74	0.8805
17:3	–0.4668	35.38	0.9616
Ti			
F127:F68 Ratio	***m* (°C/(wt.%))**	T_0 **(°C)**	R^2
14:6	–0.5886	41.91	0.8804
15:5	–0.4182	38.16	0.8413
16:4	–0.4646	35.27	0.8341
17:3	–0.4900–	31.72	0.9900

$T_0 R^2$ The fits revealed that the transition temperatures decreased with a linear tendency with microparticle concentration (wt.%). The effect of the ratio of Pluronic F127/F68 is independent of the effect of the microparticle concentration. With this it is possible to model the transition temperature with GG:Alg microparticles in Pluronic solutions, at least within the studied range of microparticle concentrations and the studied range of Pluronic F127/F68 ratios, so to determine the transition temperature to a certain microparticle concentration, there is only the need to know the transition temperature of the used Pluronic ratio.

With these data, it is possible to determine the best ratio and microparticle concentration that can be used in an injectable system. In Figure 3, lines that represent the body temperature of 37 °C and the ambient temperature of 25 °C are depicted for visual aid. For a system to be chosen, both the Ti and Tp need to be within the temperature gap of 25–37 °C. In Figure 3, the ratio of 17:3 is the ratio that meets these criteria with almost all used concentrations, excluding the concentration of 15%. With the ratio of 16:4, the microparticle concentrations of 5%, 10%, and 15% also meet the criteria. With a ratio of

15:5 only with 15% of microparticles, it was possible to have a useful injectable system. The ratio of 14:6 did not meet the criteria with any concentration. The ratio of 18:2 is not represented in Figure 3. With 0 wt.%, this ratio began the transition at 25 °C and with the introduction of microparticles further decreased the Ti, and thus it was not considered for further studies.

The presence of microparticles within Pluronic leads to an interaction between carboxylic groups of the polysaccharides and the ether groups of Pluronic, promoting the formation of a 3D structure. In addition, GG:Alg microparticles within the hydrogel might absorb water, thus decreasing the water concentration of the hydrogel and increasing the Pluronic concentration, especially the F127, which is the main contributor to the micellized form. The increase in Pluronic concentration leads to a further decrease in the transition temperatures. In a previous study [16], alginate particles within a Pluronic F127 were studied. The microparticles had a dried diameter of around 400 µm. Significant temperature decreases were obtained with the introduction of the particles to the hydrogel. The decrease of the transition temperatures with the introduction of microparticles within hydrogels has been reported in previous studies [16,32,33,36].

3.3. Frequency Sweeps at 37 °C

The dependence of G′ and G″ on the frequency of the microparticle–hydrogel system at 37 °C is presented in Figure 5. Only the ratios of 16:4 and 17:3 were chosen, since they had the most adequate transition temperatures with the microparticles. The results in Figure 5 are in accordance with Figure 4. At 37 °C, the ratio 16:4 with 0 and 2% of microparticles were not fully in the gel state, as can be observed by the lower moduli. The remaining concentrations had reached full gelation at 37 °C. Thus, with microparticle concentrations of 5, 10 and 15 wt.% (for the ratio of 16:4) the systems have their moduli within similar ranges. As observed earlier, in the temperature ramps, G″ remains higher than G′, even at the higher angular frequencies.

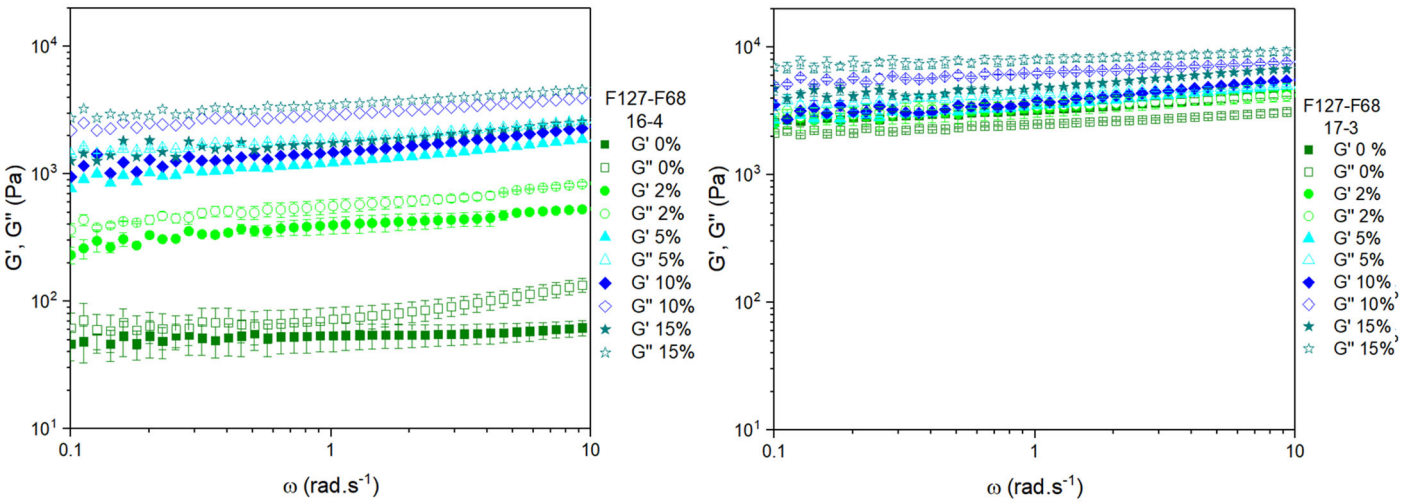

Figure 5. Frequency sweeps of the microparticle–Pluronic hydrogel composite system with different microparticle concentrations (wt.%) at 37 °C. On the (**left**), a Pluronic ratio of 16:4 and on the (**right**) of 17:3.

With a ratio of 17:3, all systems had their sol–gel transition temperatures below 37 °C, and thus all were completely in their gel state, despite the microparticles' concentration, with the moduli between 1000 and 10,000 Pa. As observed in the temperature ramps (Figure 2), the increase in microparticle concentration within the system led to higher moduli. However, G″ had a higher increase than G′. As previously said, the introduction of microparticles leads to an increase in rigidity, contributing to an increase in G′. The friction between the particles might lead to the dissipation of energy, contributing to

G″ [34,35]. Zheng et al. [35] studied the combination of polylactic-co-glycolic acid (PLGA) microparticles within a polypeptide hydrogel, and, in a dynamic temperature sweep, both moduli increased to form a gel, but with G″ > G′. Within the studied angular frequency range, this phenomenon was maintained. With an increase in microparticle concentration, the G″ was further away from G′. Thus, this phenomenon is related to the microparticle presence and not frequency. With higher particle concentration within the gap, there will be more microparticle interactions that will further increase G″ in comparison to G′, even though the system is within the gel state.

At the gel state, the hydrogel is what is considered a soft gel, with G′ and G″ parallel to each other, with a low dependency on frequency. With the introduction of the particles, the hydrogel can still be called a soft gel, since the moduli values increased and the low dependence with frequency remained. Differently from most of the literature, the G″ surpassed G′ with the introduction of the microparticles [37–39]. However, the systems were still within the gel state, since there was no decrease in the moduli. With the selected Pluronic ratios of F127:F68 of 16:4 and 17:3, at body temperature and for the majority of microparticle content, the system is in its gel state. The exceptions are for the Pluronic ratio 16:4, with 0 and 2% of microparticles, which at 37 °C were not in the gel state.

3.4. Flow Curves at 21 °C

Flow curves at 21 °C were carried out to understand if the viscosity of the gels were suitable for Pluronic-based injectable systems into the human body (Figure 6) [21]. Both 16:4 and 17:3 ratios without particles had a Newtonian behavior at 21 °C. The introduction of microparticles increased the apparent viscosity of the system, maintaining a general Newtonian behavior within the studied shear rate range. At 21 °C, both Pluronic ratios were below the transition temperatures and thus both in the sol state. The introduction of microparticles did not alter the Ti closer to 21 °C. The increase in viscosity with microparticle concentration is related to the increase in elasticity of the system. This leads to a higher resistance of flow with the applied shear rate. With 2% and 5%, the viscosity increased. For higher concentrations, especially for 15%, the increase in viscosity was more noticeable.

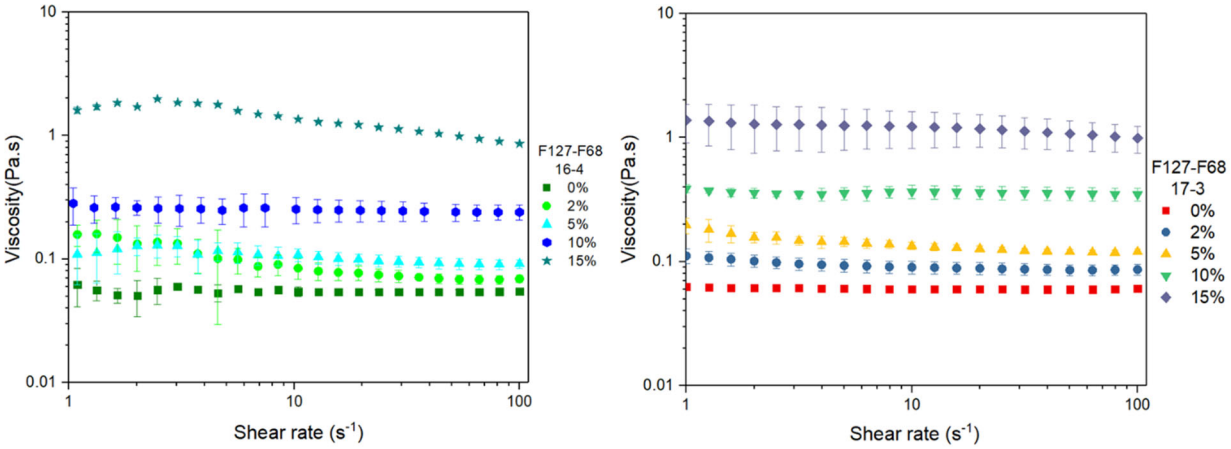

Figure 6. Flow curves of the microparticle–Pluronic hydrogel system with different microparticle concentrations (wt.%) at 21 °C. On the (**left**) is a Pluronic ratio of 16:4 and on the (**right**) of 17:3.

Below the transition temperature when the Pluronic solutions are within the sol state, they have a Newtonian behavior since the micelles are not prominent within the system. In previous studies with similar concentrations in Pluronic aqueous solutions, Newtonian behavior was also obtained at lower temperatures [20,21]. Below the gelation temperature, Pluronic systems do not exhibit any structural ordering, as observed by Shriky et al. with Rheo SANS tests [40]. With an increase in temperature, micellar formation occurs, leading to the formation of a structured system of Pluronic micelles and FCC and HC structures [22,40].

Tipa et al. [21] analyzed the injectability of similar Pluronic solutions (F127 and F68) with nanoclays. The Pluronic solutions were viable to be injected even with the introduction of the nanoclays. Similar viscosities were obtained with the GG:Alg microparticles within the Pluronic solutions, around 0.1 Pa.s, similar to the systems with 2 wt.% and 5 wt.% of this study, thus not jeopardizing the injectability of the GG:Alg microparticle–Pluronic system.

3.5. Degradation of Pluronic Hydrogels

To understand the degradation profile of Pluronic in the gel state, a solution with a ratio of 17:3 in the gel state was kept within PBS solutions with pH 7.4 and pH 6.5 for 24 h. No significant differences were observed after the first hour (Figure 7). After 3 h, the moduli had decreased but the systems were maintained within the gel state. However, with time, the moduli continued to decrease. After 6 h, the gel had almost fully degraded into the PBS solution, with only fragments of Pluronic gel dispersed within the PBS solution, which did not interfere with rheological measurements. At 24 h, the Pluronic had fully dissolved within the PBS solutions, with no fragments in the solution. There were no observed differences between the degradation of Pluronic in pH 7.4 and pH 6.5. This is because Pluronic does not have any ionizable groups within its structure [41], and thus pH will not affect the Pluronic structure or degradation.

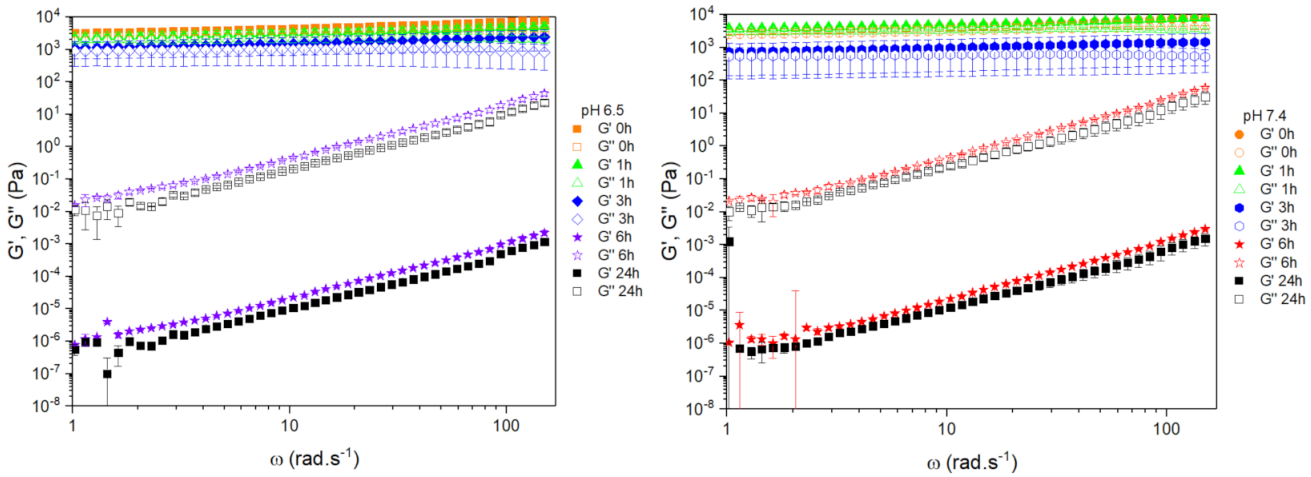

Figure 7. Frequency sweeps of Pluronic 17:3 ratio hydrogel submerged for different times in PBS with pH 6.5 (**left**) and 7.4 (**right**) at 37 °C.

With these results, it is possible to understand that the Pluronic hydrogel degrades in a matter of hours within a PBS solution, regardless of the pH (between 6.5 and 7.4). This study aimed to understand how long the structured composite system in the gel state endured within PBS and with different pH. The results suggest that the Pluronic gels dissolved within the PBS solutions, with the pH not affecting the dissolution. The amount of used PBS volume led to a fast dissolution of the Pluronic gel, reverting to the sol state. In another study, Diniz et al. [42] analyzed the degradation of Pluronic F127 within a cell culture medium (1:5 w/v): 500 µL of Pluronic within the gel state was put in contact with 1 mL of cell culture medium. After 1 week, the hydrogel had fragmented into small pieces, and 85% of the initial weight had disappeared in 2 weeks. The fragmentation of the hydrogel also occurred in our degradation, though, at a much faster rate due to the ratio between Pluronic and PBS solution. The in vivo environment differs from the in vitro tests that were done. Heo et al. [43] studied PLGA microspheres within a Pluronic aqueous solution (20 wt.%). The Pluronic hydrogel only disappeared after 6 days in vivo. With the microparticles within the Pluronic, the hydrogel also disappeared after 7 days. This shows that the Pluronic hydrogel is capable of withstanding more than some hours in vivo. Our test demonstrated that there were no rheological differences between pH 6.5 and 7.4. Further studies with similar conditions to the in vivo environment need to be carried out.

3.6. In Vitro MB-Release Profiles

The MB-loaded hydrogel had fully released the MB by 6 h (Figure 8a). The complete release from the hydrogel correlates with the hydrogel's degradation in PBS. The hydrogel had almost fully degraded by 6 h in PBS. In addition, similarly to the degradation trials, the pH did not affect the release of MB due to the same reasons previously mentioned [41]. In Figure 8b, it can be observed that there are no significant differences between the release profiles of microparticles alone and the microparticles embedded within the hydrogel during the full-term release. Within the first six hours, when the hydrogel was still present around the microparticles, the release profile was similar to the microparticles for the 16:4 ratio. However, with the 17:3 ratio, there was a slightly slower release profile (Figure 8b). The used ratio of hydrogel affected the release profile during the first 6 h. Afterwards, no differences between the 17:3 and 16:4 ratios were observed. Since the hydrogel dissolved within 6 h, the release of MB after that is similar to that of the microparticles. The pH affected the release from the microparticles, as was observed in our previous study [25]. The concentration of microparticle and, thus the amount of hydrogel that embedded the microparticles did not affect microparticle release either, since there were no differences between the 2% and 5% microparticle concentrations (Figure 8c). Thus, the addition of Pluronic around the microparticles did not alter the release profiles from the microparticles within the studied conditions.

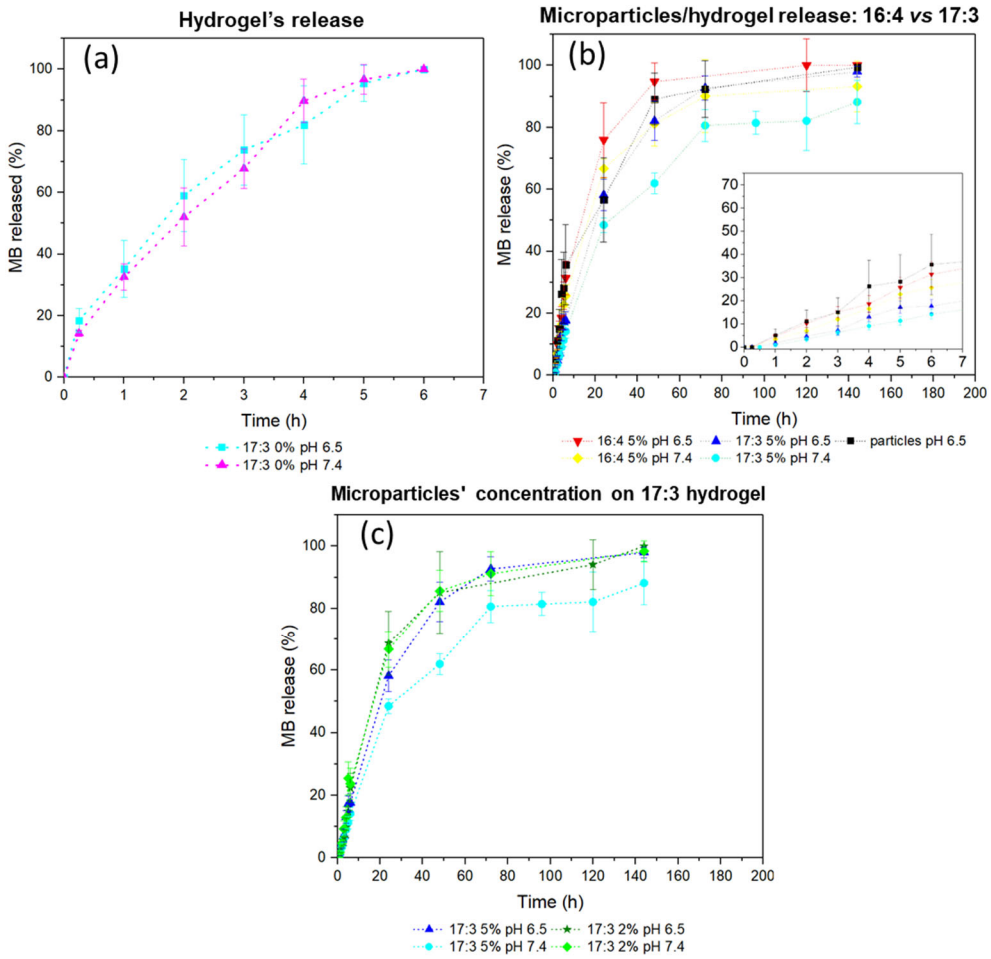

Figure 8. (**a**) Release profile of MB-loaded Pluronic hydrogel, 17:3 F127:F68 ratio, in PBS pH 6.5 and pH 7.4; (**b**) Release profiles of microparticles (in PBS pH 6.5) and microparticle–hydrogel composite system for 16:4 and 17:3 F127:F68 ratios (5 wt.% of microparticles) in PBS pH 6.5 and pH 7.4; (**c**) Release profile of microparticle–hydrogel composite system with F127:F68 ratio 17:3 with 2 wt.% and 5 wt.% microparticles in PBS pH 6.5 and pH 7.4.

In previous studies [24], the release profiles of drug-loaded microparticles within hydrogels revealed that the hydrogels had a delaying effect on the release profile. With Dex-loaded PLGA microspheres in Pluronic, in vivo studies were reported in [43]. Pluronic had a delaying effect on the initial burst release. Possibly due to the interaction between Dex and the hydrogel. More release studies need to be done with similar conditions to the in vivo environment to understand if the Pluronic hydrogel does not affect the GG:Alg microparticles MB release. This system can also serve as a dual-drug-delivery system. Zheng et al. [35] developed a polypetide hydrogel with combretastatin A-4 (CA-4) and PLGA microspheres loaded with docetaxel (Dtx). Dual-release profiles were achieved, where the CA-4 was first released from the hydrogel followed by the Dtx from the microspheres, for a more synergetic treatment. In addition, as previously referenced, Ma et al. [4] used dual-release systems using microparticle–hydrogel systems for sequential drug delivery for skin treatments.

It was possible to develop a dual-release DDS that is able to rapidly release a first drug contained within the hydrogel, followed by the release of a second drug with a more sustainable release profile contained within the microparticles. It is then possible to adjust this DDS for complex therapeutic systems that require this type of dual-release profile.

3.7. Mathematical Fittings

For mathematical model fitting of the MB-release profiles, a modified Korsmeyer–Peppas (KP) model (Equation (2)) and a modified Peppas–Sahlin (PS) model (Equation (3)) were chosen. In the modified Korsmeyer–Peppas model, Q_t is the drug concentration released at each time (t), k is a structural factor, n is related to the release mechanism and T_{lag} is the lag time before drug release [44]. Fickian diffusion occurs if $n \leq 0.43$. In this type of release, diffusion is the main process of the drug molecules passing to the release medium. If $n = 0.85$, a case II transport occurs, in which the release is mainly controlled by swelling and relaxation [45]. Anomalous transport, a mix of the previous ones, occurs between the previous two ($n \in [0.43, 0.85]$). With $n > 0.85$, super case II transport occurs. With this last one, the release is affected by the mobility of the polymeric chains and by erosion [45,46]. The modified Peppas–Sahlin model (PS) uses two constants, k_1 and k_2. k_1 correlates with the Fickian diffusion and k_2 with case II transport [47]. The exponent m can be associated with parameter n of the KP model [48]. Similar to the modified KP model, T_{lag} is also accounted for. Table 2 presents the models' parameters and adjusted R^2 (R^2_{adj}) given by the DDSolver program.

$$Q_t = k\left(t - T_{lag}\right)^n \tag{2}$$

$$Q_t = k_1\left(t - T_{lag}\right)^{2m} + k_2\left(t - T_{lag}\right)^{2m} \tag{3}$$

Table 2. Parameters obtained from the drug-release fittings.

Batches (g)/pH		16:4 5%		17:3 5%		17:3 2%		Microparticles
		pH 6.5	pH 7.4	pH 6.5	pH 7.4	pH 6.5	pH 7.4	pH 6.5
KP T_{lag}	**k**	21.150	22.533	20.995	20.710	23.236	21.849	30.191
	n	0.349	0.309	0.331	0.298	0.312	0.325	0.240
	T_{lag}	1.938	2.923	3.868	3.896	3.959	2.957	2.957
	R^2adj	0.929	0.956	0.965	0.956	0.955	0.961	0.955
PS T_{lag}	**k_1**	10.316	12.253	9.105	7.820	8.011	11.780	13.744
	k_2	–0.245	–0.389	–0.205	–0.178	–0.158	–0.345	–0.446
	m	0.691	0.593	0.658	0.670	0.730	0.606	0.557
	T_{lag}	0.835	1.746	2.330	1.791	1.872	1.894	0.893
	R^2adj	0.995	0.994	0.997	0.996	0.989	0.991	0.990

Using the KP T_{lag} model and the SP T_{lag} model, good fits were obtained for the microparticle–hydrogel system and for the microparticles alone. Higher values of R^2_{adj} were obtained with the PS T_{lag} model, indicating a better fit with this last model. With the KP T_{lag} model, all values of parameter n were below 0.43, thus indicating a Fickian release. However, with the PS model, parameter m values were above 0.43, thus having a mixed contribution of a Fickian release profile and a case II transport profile. This occurred for the system with and without hydrogel. However, with the PS model, the contribution of k_1 was significantly above k_2, thus indicating a higher contribution from a Fickian release profile than a case II transport.

The obtained parameters with the 17:3 ratio were smaller than with 16:4, possibly related to the slower earlier release observed in Figure 8b. The pH did not affect MB release from plain hydrogels, since no differences are observed in Table 2 and Figure 8. However, the pH did affect the microparticle-release profile, as previously studied [25]. With the KP T_{lag} model, the k value of microparticles alone (pH 6.5) was higher than k values with the hydrogel. This might be associated with the initial burst release. The hydrogel delayed the initial burst release, thus having a higher k value for the microparticles alone. This early delay can be observed in Figure 8b.

The obtained profiles were similar to the ones obtained in the previous study, with only the microparticles showing a predominately Fickian release profile. The hydrogel had an effect on the early release of the microparticles but not during all the release time. This is largely due to the fact that the hydrogel rapidly disintegrated within the PBS solutions.

4. Conclusions

This study aimed to develop a microparticle–hydrogel injectable DDS made of gellan gum/alginate microparticles and Pluronic hydrogel. The most suitable ratios of Pluronic F127 and F68 for different microparticle concentrations were found using rheological characterization. The decrease in F127 and increase in F68 in an aqueous solution (total polymer content of 20 wt.%) increased the sol–gel transition temperature. The introduction of microparticles led to a decrease in sol–gel transition temperatures. The optimized system with a 17:3 ratio with microparticles was found to be in the sol state at 21 °C and in the gel state at 37 °C, ideal for injectable DDSs. At 37 °C, the microparticle presence, within the scope of the studied concentrations, did not alter the modulus of the hydrogel. Here, we developed a dual-release DDS that is able to deliver drugs at different stages of treatment. The hydrogel released MB within hours, while microparticles had a more prolonged release profile. This phenomenon is suitable for possible dual-release DDSs. The hydrogel affected the release profile of the microparticles during the first release hours for the 17:3 ratio. More studies need to be performed in conditions similar to the in vivo environment. Release trials with more drugs will be performed to understand the release profiles of the systems. Cytotoxic tests will also be performed to understand if the system presents toxicity. Release trials and biodegradation trials with conditions more similar to the in vivo environment will be carried out before proceeding to in vivo trials. With this study, a potential dual-release system with rapid release followed by more controlled release was developed for potential biomedical applications.

Author Contributions: Conceptualization, H.C., P.I.P.S., J.P.B. and M.T.C.; methodology, H.C. and A.R.E.; validation, H.C. and A.R.E.; formal analysis, H.C. and A.R.E.; writing—original draft preparation, H.C.; writing—review and editing, H.C., P.I.P.S., J.P.B. and M.T.C.; visualization, H.C.; supervision, P.I.P.S., J.P.B. and M.T.C. All authors have read and agreed to the published version of themanuscript.

Funding: This work was financed by national funds from FCT-Fundação para a Ciência e a Tecnologia, I.P., in the scope of the projects LA/P/0037/2020, UIDP/50025/2020 and UIDB/50025/2020 of the Associate Laboratory Institute of Nanostructures, Nanomodelling and Nanofabrication–i3N. H.C. acknowledges FCT for the PhD grant with reference SFRH/BD/144986/2019 and P.S. acknowledges the individual contract CEECIND. 03189.2020.

Conflicts of Interest: The authors declare no conflict of interest.

References

1. Patra, J.K.; Das, G.; Fraceto, L.F.; Campos, E.V.R.; del Pilar Rodriguez-Torres, M.; Acosta-Torres, L.S.; Diaz-Torres, L.A.; Grillo, R.; Swamy, M.K.; Sharma, S.; et al. Nano based drug delivery systems: Recent developments and future prospects. *J. Nanobiotechnol.* **2018**, *16*, 71. [CrossRef] [PubMed]
2. Mura, S.; Nicolas, J.; Couvreur, P. Stimuli-responsive nanocarriers for drug delivery. *Nat. Mater.* **2013**, *12*, 991–1003. [CrossRef] [PubMed]
3. Ahmed, E.M. Hydrogel: Preparation, characterization, and applications: A review. *J. Adv. Res.* **2015**, *6*, 105–121. [CrossRef] [PubMed]
4. Ma, Z.; Song, W.; He, Y.; Li, H. Multilayer Injectable Hydrogel System Sequentially Delivers Bioactive Substances for Each Wound Healing Stage. *ACS Appl. Mater. Interfaces* **2020**, *12*, 29787–29806. [CrossRef]
5. Zhu, Y.; Kong, L.; Farhadi, F.; Xia, W.; Chang, J.; He, Y.; Li, H. An injectable continuous stratified structurally and functionally biomimetic construct for enhancing osteochondral regeneration. *Biomaterials* **2018**, *192*, 149–158. [CrossRef]
6. Li, X.; He, Y.; Hou, J.; Yang, G.; Zhou, S. A Time-Programmed Release of Dual Drugs from an Implantable Trilayer Structured Fiber Device for Synergistic Treatment of Breast Cancer. *Small* **2019**, *16*, 1902262. [CrossRef]
7. Yu, H.; Ning, N.; Meng, X.; Chittasupho, C.; Jiang, L.; Zhao, Y. Sequential Drug Delivery in Targeted Cancer Therapy. *Pharmaceutics* **2022**, *14*, 573. [CrossRef]
8. Zhang, H.; Cheng, J.; Ao, Q. Preparation of Alginate-Based Biomaterials and Their Applications in Biomedicine. *Mar. Drugs* **2021**, *19*, 264. [CrossRef]
9. de Farias, A.L.; Meneguin, A.B.; Barud, H.D.S.; Brighenti, F.L. The role of sodium alginate and gellan gum in the design of new drug delivery systems intended for antibiofilm activity of morin. *Int. J. Biol. Macromol.* **2020**, *162*, 1944–1958. [CrossRef]
10. Mun, S.; Kim, H.C.; Yadave, M.; Kim, J. Graphene oxide–gellan gum–sodium alginate nanocomposites: Synthesis, characterization, and mechanical behavior. *Compos. Interfaces* **2015**, *22*, 249–263. [CrossRef]
11. Rosas-Flores, W.; Ramos-Ramírez, E.G.; Salazar-Montoya, J.A. Microencapsulation of Lactobacillus helveticus and Lactobacillus delbrueckii using alginate and gellan gum. *Carbohydr. Polym.* **2013**, *98*, 1011–1017. [CrossRef] [PubMed]
12. Chen, M.-J.; Chen, K.-N.; Kuo, Y.-T. Optimal thermotolerance ofBifidobacterium bifidum in gellan–alginate microparticles. *Biotechnol. Bioeng.* **2007**, *98*, 411–419. [CrossRef] [PubMed]
13. Jana, S.; Das, A.; Nayak, A.K.; Sen, K.K.; Basu, S.K. Aceclofenac-loaded unsaturated esterified alginate/gellan gum microspheres: In vitro and in vivo assessment. *Int. J. Biol. Macromol.* **2013**, *57*, 129–137. [CrossRef] [PubMed]
14. Larrañeta, E.; Stewart, S.; Ervine, M.; Al-Kasasbeh, R.; Donnelly, R.F. Hydrogels for Hydrophobic Drug Delivery. Classification, Synthesis and Applications. *J. Funct. Biomater.* **2018**, *9*, 13. [CrossRef] [PubMed]
15. Hoffman, A.S. Hydrogels for biomedical applications. *Adv. Drug Deliv. Rev.* **2012**, *64*, 18–23. [CrossRef]
16. Cidade, M.; Ramos, D.J.; Santos, J.; Carrelo, H.; Calero, N.; Borges, J.P. Injectable Hydrogels Based on Pluronic/Water Systems Filled with Alginate Microparticles for Biomedical Applications. *Material* **2019**, *12*, 1083. [CrossRef]
17. Calero, N.; Santos, J.; Echevarría, C.; Muñoz, J.; Cidade, M.T. Time-dependent behavior in analyte-, temperature-, and shear-sensitive Pluronic PE9400/water systems. *Colloid Polym. Sci.* **2018**, *296*, 1515–1522. [CrossRef]
18. Klouda, L.; Mikos, A.G. Thermoresponsive hydrogels in biomedical applications. *Eur. J. Pharm. Biopharm.* **2008**, *68*, 34–45. [CrossRef]
19. Chatterjee, S.; Hui, P.C.-L.; Kan, C.-W. Thermoresponsive Hydrogels and Their Biomedical Applications: Special Insight into Their Applications in Textile Based Transdermal Therapy. *Polymers* **2018**, *10*, 480. [CrossRef]
20. Jalaal, M.; Cottrell, G.; Balmforth, N.; Stoeber, B. On the rheology of Pluronic F127 aqueous solutions. *J. Rheol.* **2017**, *61*, 139–146. [CrossRef]
21. Tipa, C.; Cidade, M.T.; Vieira, T.; Silva, J.C.; Soares, P.I.P.; Borges, J.P. A New Long-Term Composite Drug Delivery System Based on Thermo-Responsive Hydrogel and Nanoclay. *Nanomaterials* **2020**, *11*, 25. [CrossRef] [PubMed]
22. Zhang, M.; Djabourov, M.; Bourgaux, C.; Bouchemal, K. Nanostructured fluids from pluronic®mixtures. *Int. J. Pharm.* **2013**, *454*, 599–610. [CrossRef] [PubMed]
23. Rio, L.G.-D.; Diaz-Rodriguez, P.; Landin, M. New tools to design smart thermosensitive hydrogels for protein rectal delivery in IBD. *Mater. Sci. Eng. C* **2020**, *106*, 110252. [CrossRef]
24. Carrêlo, H.; Soares, P.I.P.; Borges, J.P.; Cidade, M.T. Injectable Composite Systems Based on Microparticles in Hydrogels for Bioactive Cargo Controlled Delivery. *Gels* **2021**, *7*, 147. [CrossRef]
25. Carrêlo, H.; Cidade, M.T.; Borges, J.P.; Soares, P.I.P. Gellan gum/alginate microparticles as drug delivery vehicles: DOE production optimization and drug delivery. *Submited* **2022**.
26. Nastase, I.; Croitoru, C.V.; Vartires, A.; Tataranu, L. Indoor Environmental Quality in Operating Rooms: An European Standards Review with Regard to Romanian Guidelines. *Energy Procedia* **2016**, *85*, 375–382. [CrossRef]
27. Li, T.; Bao, Q.; Shen, J.; Lalla, R.V.; Burgess, D.J. Mucoadhesive in situ forming gel for oral mucositis pain control. *Int. J. Pharm.* **2020**, *580*, 119238. [CrossRef]
28. Suman, K.; Sourav, S.; Joshi, Y.M. Rheological signatures of gel–glass transition and a revised phase diagram of an aqueous triblock copolymer solution of Pluronic F127. *Phys. Fluids* **2021**, *33*, 073610. [CrossRef]
29. Costanzo, S.; Di Sarno, A.; D'Apuzzo, M.; Avallone, P.R.; Raccone, E.; Bellissimo, A.; Auriemma, F.; Grizzuti, N.; Pasquino, R. Rheology and morphology of Pluronic F68 in water. *Phys. Fluids* **2021**, *33*, 043113. [CrossRef]

30. Lee, M.H.; Shin, G.H.; Park, H.J. Solid lipid nanoparticles loaded thermoresponsive pluronic-xanthan gum hydrogel as a transdermal delivery system. *J. Appl. Polym. Sci.* **2017**, *135*, 46004. [CrossRef]
31. Delgado, B.; Carrêlo, H.; Loureiro, M.V.; Marques, A.C.; Borges, J.P.; Cidade, M.T. Injectable hydrogels with two different rates of drug release based on pluronic/water system filled with poly(ε-caprolactone) microcapsules. *J. Mater. Sci.* **2021**, *56*, 13416–13428. [CrossRef]
32. Lin, H.-R.; Sung, K.C.; Vong, W.-J. In Situ Gelling of Alginate/Pluronic Solutions for Ophthalmic Delivery of Pilocarpine. *Biomacromolecules* **2004**, *5*, 2358–2365. [CrossRef] [PubMed]
33. Rueda, M.M.; Auscher, M.-C.; Fulchiron, R.; Périé, T.; Martin, G.; Sonntag, P.; Cassagnau, P. Rheology and applications of highly filled polymers: A review of current understanding. *Prog. Polym. Sci.* **2016**, *66*, 22–53. [CrossRef]
34. Bek, M.; Gonzalez-Gutierrez, J.; Kukla, C.; Črešnar, K.P.; Maroh, B.; Perše, L.S. Rheological Behaviour of Highly Filled Materials for Injection Moulding and Additive Manufacturing: Effect of Particle Material and Loading. *Appl. Sci.* **2020**, *10*, 7993. [CrossRef]
35. Zheng, Y.; Cheng, Y.; Chen, J.; Ding, J.; Li, M.; Li, C.; Wang, J.-C.; Chen, X. Injectable Hydrogel–Microsphere Construct with Sequential Degradation for Locally Synergistic Chemotherapy. *ACS Appl. Mater. Interfaces* **2017**, *9*, 3487–3496. [CrossRef]
36. Chatterjee, S.; Hui, P.C.L.-I. Review of Applications and Future Prospects of Stimuli-Responsive Hydrogel Based on Thermo-Responsive Biopolymers in Drug Delivery Systems. *Polymers* **2021**, *13*, 2086. [CrossRef]
37. Zarandona, I.; Bengoechea, C.; Álvarez-Castillo, E.; de la Caba, K.; Guerrero, A.; Guerrero, P. 3D Printed Chitosan-Pectin Hydrogels: From Rheological Characterization to Scaffold Development and Assessment. *Gels* **2021**, *7*, 175. [CrossRef]
38. Ghanbari, M.; Salavati-Niasari, M.; Mohandes, F.; Dolatyar, B.; Zeynali, B. *In vitro* study of alginate–gelatin scaffolds incorporated with silica NPs as injectable, biodegradable hydrogels. *RSC Adv.* **2021**, *11*, 16688–16697. [CrossRef]
39. Liu, Y.; Yu, Y.; Liu, C.; Regenstein, J.M.; Liu, X.; Zhou, P. Rheological and mechanical behavior of milk protein composite gel for extrusion-based 3D food printing. *LWT* **2018**, *102*, 338–346. [CrossRef]
40. Shriky, B.; Kelly, A.; Isreb, M.; Babenko, M.; Mahmoudi, N.; Rogers, S.; Shebanova, O.; Snow, T.; Gough, T. Pluronic F127 thermosensitive injectable smart hydrogels for controlled drug delivery system development. *J. Colloid Interface Sci.* **2019**, *565*, 119–130. [CrossRef]
41. Park, S.Y.; Lee, Y.; Bae, K.H.; Ahn, C.-H.; Park, T.G. Temperature/pH-Sensitive Hydrogels Prepared from Pluronic Copolymers End-Capped with Carboxylic Acid Groups via an Oligolactide Spacer. *Macromol. Rapid Commun.* **2007**, *28*, 1172–1176. [CrossRef]
42. Diniz, I.M.A.; Chen, C.; Xu, X.; Ansari, S.; Zadeh, H.H.; Marques, M.M.; Shi, S.; Moshaverinia, A. Pluronic F-127 hydrogel as a promising scaffold for encapsulation of dental-derived mesenchymal stem cells. *J. Mater. Sci. Mater. Med.* **2015**, *26*, 153. [CrossRef] [PubMed]
43. Heo, J.Y.; Noh, J.H.; Park, S.H.; Ji, Y.B.; Ju, H.J.; Kim, D.Y.; Lee, B.; Kim, M.S. An Injectable Click-Crosslinked Hydrogel that Prolongs Dexamethasone Release from Dexamethasone-Loaded Microspheres. *Pharmaceutics* **2019**, *11*, 438. [CrossRef] [PubMed]
44. Zhang, Y.; Huo, M.; Zhou, J.; Zou, A.; Li, W.; Yao, C.; Xie, S. DDSolver: An Add-In Program for Modeling and Comparison of Drug Dissolution Profiles. *AAPS J.* **2010**, *12*, 263–271. [CrossRef] [PubMed]
45. Prezotti, F.G.; Cury, B.S.F.; Evangelista, R.C. Mucoadhesive beads of gellan gum/pectin intended to controlled delivery of drugs. *Carbohydr. Polym.* **2014**, *113*, 286–295. [CrossRef] [PubMed]
46. Costa, P.; Lobo, J.M.S. Modeling and comparision of dissolution profiles. *Eur. J. Pharm. Sci.* **2001**, *13*, 123–124.
47. Arifin, D.Y.; Lee, L.Y.; Wang, C.-H. Mathematical modeling and simulation of drug release from microspheres: Implications to drug delivery systems. *Adv. Drug Deliv. Rev.* **2006**, *58*, 1274–1325. [CrossRef]
48. Peppas, N.A.; Sahlin, J.J. A simple equation for the description of solute release. III. Coupling of diffusion and relaxation. *Int. J. Pharm.* **1989**, *57*, 169–172. [CrossRef]